Characterization of MTMR3: an inositol lipid 3-phosphatase with novel substrate specificity

Donna M. Walker*§, Sylvie Urbé*§, Stephen K. Dove†, Danielle Tenza‡, Graça Raposo‡ and Michael J. Clague*

Inositol lipids play key roles in many fundamental cellular processes that include growth, cell survival, motility, and membrane trafficking. Recent studies on the PTEN and Myotubularin proteins have underscored the importance of inositol lipid 3-phosphatases in cell function. Inactivating mutations in the genes encoding PTEN and Myotubularin are key steps in the progression of some cancers and in the onset of X-linked myotubular myopathy, respectively. Myotubularin-related protein 3 (MTMR3) shows extensive homology to Myotubularin, including the catalytic domain, but additionally possesses a C-terminal extension that includes a FYVE domain. We show that MTMR3 is an inositol lipid 3-phosphatase, with a so-far-unique substrate specificity. It is able to hydrolyze PtdIns3*P* and PtdIns(3,5)P_2, both in vitro and when heterologously expressed in *S. cerevisiae*, and to thereby provide the first clearly defined route for the cellular production of PtdIns5*P*. Overexpression of a catalytically dead MTMR3 (C413S) in mammalian cells induces a striking formation of vacuolar compartments that enclose membranous structures that are highly concentrated in mutant proteins.

Addresses: *Physiological Laboratory, University of Liverpool, Crown Street, Liverpool L69 3BX, United Kingdom. †Department of Biosciences, University of Birmingham, The Medical School, Birmingham B15-2TT, United Kingdom. ‡Institut Curie, Centre National de la Recherche Scientifique UMR 144, 75005 Paris, France.

Correspondence: Michael J. Clague
E-mail: clague@liv.ac.uk

§These authors contributed equally to this study.

Received: **11 July 2001**
Revised: **6 August 2001**
Accepted: **30 August 2001**

Published: **16 October 2001**

Current Biology 2001, 11:1600–1605

0960-9822/01/$ – see front matter

Results and discussion

Myotubularin is a phosphoinositide 3-phosphatase that defines a family of at least nine proteins in man [1]. The Cx_5R active site motif (CSDGWDR) differs from that of the polyphosphoinositide (PPI) 3-phosphatase PTEN in that, rather than containing two basic residues, it contains two conserved aspartate residues. In this respect, it more closely resembles the Sac1 phosphoinositide phosphatase from *Saccharomyces cerevisiae* (CMDCLDR) whose likely physiological target is PtdIns4*P* [2]. MTMR3 shares homology with Myotubularin over its phosphatase domain, but it also contains additional structural features (Figure 1) that include a FYVE domain toward its C terminus and a putative PH domain, N-terminal to its catalytic domain (Tobias Doerks, EMBL, personal communication). Our initial attempts to express GST-MTMR3 in bacteria (full-length form or MTMR3 [1–488]) were unsuccessful owing to degradation and insolubility of the protein. Expression of soluble protein was achieved with baculovirus-infected Sf9 cells, in which we obtained up to 50% of expressed MTMR3 in the soluble fraction. We incubated the enzyme with diC16-phosphatidylinositols and monitored the liberation of free phosphate by using a malachite green colorimetric assay [3]. Under the experimental conditions used, significant activity was detected against only two of seven potential PPI substrates, PtdIns3*P* and PtdIns(3,5)P_2 (Figure 2). This activity was mirrored by HA-tagged MTMR3 immunoprecipitated from transfected Hela cells (not shown). Activity was not registered by a C-terminally truncated form of MTMR3 (1–488) that lacks most of the wild-type protein, including the FYVE domain, or in a point mutant in which the active site cysteine is mutated to serine (C413S, not shown). 10 mM EDTA, which should disrupt the structure of the FYVE domain by chelation of zinc and thereby abrogate PtdIns3*P* binding, did not reduce phosphatase activity against PtdIns3*P*. No phosphatase activity was detected against *para*-nitrophenylphosphate (pNPP) at pH 7.2, although it has previously been shown that this enzyme possesses dual-specificity phosphatase activity against proteins [4]. The in vitro specificity of the lipid phosphatase activity toward PtdIns3*P* and PtdIns(3,5)P_2 distinguishes MTMR3 from other 3-phosphatases, Myotubularin, which is selective for PtdIns3*P*, and PTEN, which displays minimal selectivity in vitro, although its tumor suppressor function is presumably due to attenuation of $PtdInsP_3$ signaling [1].

The yeast strain *S. cerevisiae* possesses no obvious homolog of MTMR3. We transfected yeast with expression constructs for either wild-type MTMR3 or the phosphatase dead form MTMR3 (C413S). The resultant yeast cells were first examined morphologically. Both appeared

Figure 1

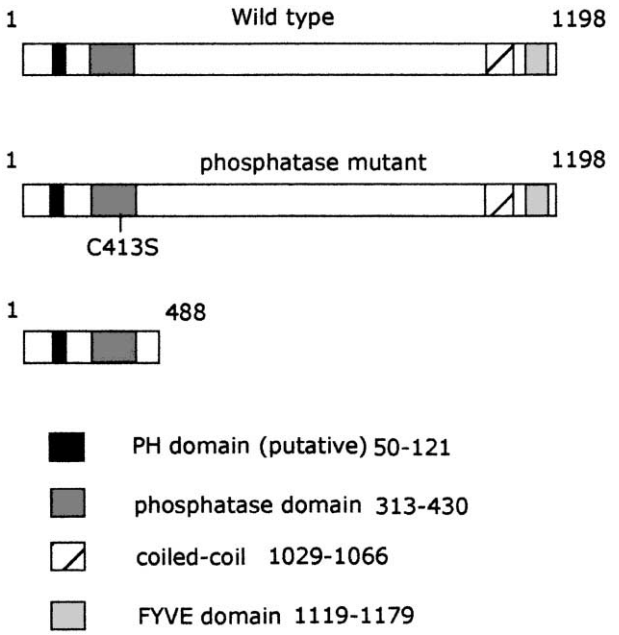

Domain structure of MTMR3. Schematic representation of proposed MTMR3 domain structure and of point mutant and truncation protein constructs used in this study.

Figure 2

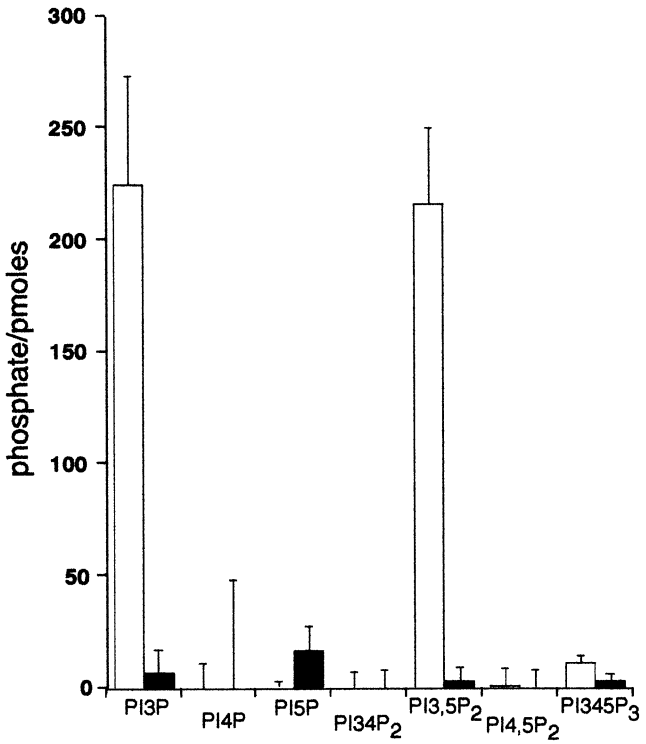

Phosphoinositide phosphatase activity of MTMR3. Full-length MTMR3 (white bars) or MTMR3 (1-488) (black bars) were contemporaneously prepared as GST-tagged fusion proteins from Sf9 cells. Equimolar quantities of enzyme were incubated with potential phosphatidylinositol substrates for 10 min at room temperature as described in Materials and Methods. Liberation of free phosphate was determined with the Malachite Green assay described and is expressed as mOD units. Significant activity was found for full-length protein with PI3P and PI(3,5)P_2.

larger than control cells (Figure 3). MTMR3-yeast showed an enlarged vacuole, reminiscent of Δ*fab1* cells [5], while MTMR3(C413S) produced a collection of smaller vesicle profiles within the cell lumen (Figure 3).

Yeast cells normally have low levels of PtdIns(3,5)P_2 but no detectable levels of PtdIns5*P* (Figure 4a). PtdIns5*P* has been shown to be represented at detectable levels in fibroblasts [6], but a cellular pathway for the production of this lipid has not been hitherto described. A PtdIns 5-kinase (PIKfyve) has been identified, but available evidence suggests that its physiological substrate is PtdIns3*P* rather than PtdIns [7, 8].

In yeast expressing MTMR3, an additional peak on the HPLC gradient used to separate Gro*P*Ins*P*s is evident (Figure 4c); this peak is not produced in cells expressing the phosphatase dead mutant MTMR3 (C413S) (Figure 4e). This peak migrates fractionally more slowly than PtdIns4*P*. We suspected that this may correspond to PtdIns5*P* produced from the phosphatase activity of MTMR3 exerted on PtdIns(3,5)P_2. This was confirmed by the finding that the emergent peak exactly comigrated with a Gro*P*Ins5*P* standard (Figure 5a). Accordingly, the PtdIns5*P* peak increased in MTMR3-expressing cells that were subjected to osmotic stress, owing to enhanced levels of PtdIns(3,5)P_2 substrate [9], but was not observed in MTMR3(C413S)-expressing cells despite increased levels of PtdIns(3,5)P_2 (Figure 4f).

PtdIns(3,5)P_2 is produced in yeast by the action of the PtdIns3*P* 5-kinase Fab1 [10]. Δ*fab1* cells are unable to produce PtdIns(3,5)P_2 basally or in response to osmotic shock. In these cells MTMR3 is also unable to promote the formation of PtdIns5*P*, confirming PtdIns(3,5)P_2 as the relevant substrate for MTMR3 phosphatase activity (Figure 5b). It is also evident that MTMR3 activity leads to reduced levels of PtdIns3*P* as predicted from in vitro data, although we are not able to definitively say whether this is due to a direct action on PtdIns3*P* or to increased PtdIns(3,5)P_2 turnover.

We have analyzed the sub-cellular distribution of epitope-tagged MTMR3. The wild-type protein is largely cytosolic, but both punctate and reticular staining (which overlaps with the ER marker calnexin) are also evident (see Figures S1 and S2 available with this article on the internet). Unusually for a FYVE domain-containing protein, no colocalization with endosomal markers could be found. A point mutation (C413S) at the active site of the phospha-

Figure 3

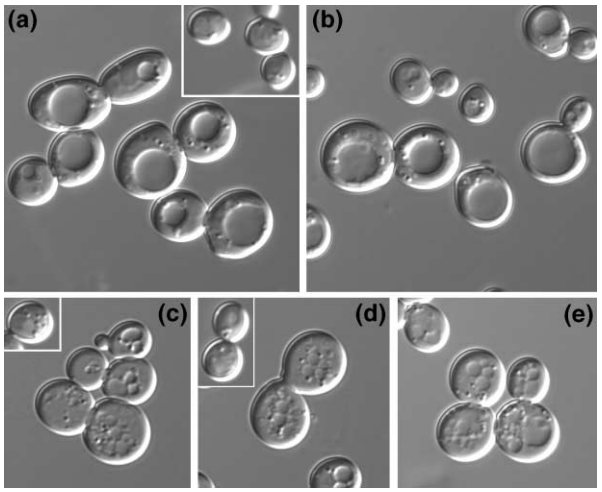

Modification of yeast morphology by MTMR3 expression. Yeast cells expressing **(a,b)** human MTMR3 have an aberrantly large vacuole, while cells expressing **(c–e)** the phosphatase dead mutant MTMR3 (C413S) contain a collection of smaller vacuolar structures. The parental yeast wild-type strain (BY4742) is shown in insets for comparison.

Figure 4

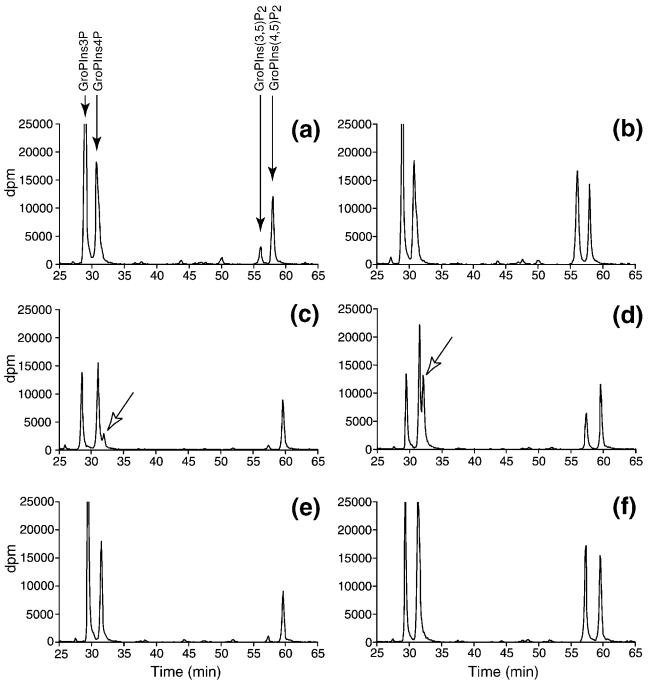

Modification of yeast phosphatidylinositol lipid composition by MTMR3 expression. HPLC separations of deacylated inositol lipids from [^{3}H] *myo*-inositol radiolabeled yeast strains expressing **(a,b)** GFP, **(c,d)** GFP-MTMR3, or **(e,f)** GFP-MTMR3 C413S. The cells were either (a,c,e) unstressed or (b,d,f) incubated in 0.9 M NaCl for 10 min prior to killing and lipid extraction. The glycero-phosphoinositols were then resolved on the HPLC gradient of Stephens et al. [18]. The *x* axis represents retention time in minutes, while the *y* axis shows the radioactivity eluting from the column in dpm. The additional Gro*P*Ins5*P* peak observed in GFP-MTMR3-expressing cells is indicated by white arrows in (c) and (d).

tase domain ablates enzyme activity in vitro (not shown) and in yeast (Figure 4e). When it was expressed in HeLa cells, we found that the mutant protein provided a staining pattern that was significantly different from that of the active enzyme. Cytosolic staining was not evident, while bright fluorescent clusters and punctae were much more pronounced (see Figure S2 in the Supplementary material). Electron microscopic examination revealed the subcellular localization at high resolution of the wild-type and the mutant protein. Immunogold labeling of ultrathin cryosections showed that the wild-type protein was in the cytosol but also concentrated at the cytosolic face of membranous structures (Figure 6a). These labeled membranes are poorly defined morphologically but are dispersed throughout the cell. In contrast, the C413S mutant was found most frequently accumulated in internal membranes of 200–350 nm compartments that appeared to contain both cytosol and lysosome-like structures. The limiting membrane, which engulfs these components, was mostly free of gold particles (Figure 6b). These structures are only induced by C413S protein expression and could be observed throughout the cell. Morphologically they resemble autophagosomes.

Autophagy is a fairly mysterious process in mammalian cells, at the molecular level, although recent progress in yeast has been very rapid [11, 12]. Classically it is induced by nutrient deprivation. It is a multi-step process that involves the bulk sequestration of both cytoplasm and membrane-bounded organelles and that ultimately leads to the degradation of autophagocytosed material after fusion with lysosomes. It has been suggested that the ER provides the membrane that wraps around cytosol and organelles in the initial step of autophagosome formation [12].

Previous studies have identified a link between autophagy and PPI metabolism. PtdIns 3-kinase activity, leading to the generation of PtdIns3*P*, is required for autophagy in both yeast and mammalian cells [13, 14]. Note that this requirement would be a prerequisite for regulation of autophagy via the phosphoinositide phosphatase activity of MTMR3.

How then might phosphatase-inactive MTMR3 operate on a pathway of organelle biogenesis in mammalian cells as seen in Figure 6b? One possibility is that MTMR3 (C413S) can act either as a substrate trap or as a dominant-negative mutant that inhibits endogenous enzyme activity. Local accumulation of this substrate or the failure to generate breakdown products at the appropriate location may then lead to the observed morphological changes.

Figure 5

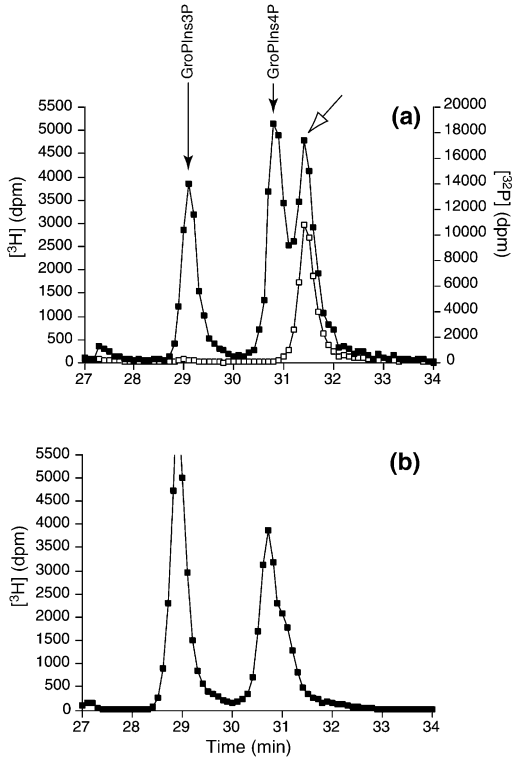

Cochromatography of the novel inositol lipid made by MTMR3 in yeast with an authentic [^{32}P]Gro*P*Ins5*P* standard. A **(a)** wild-type or **(b)** *fab1* deletion strain expressing GFP-MTMR3 was radiolabeled with [^{3}H]inositol for five divisions and then incubated with 0.9 M NaCl for 10 min before being killed with acidified methanol. The [^{3}H]lipids were extracted and deacylated (see Materials and methods), and authentic [^{32}P]Gro*P*Ins5*P* was added. The glycero-phosphoinositols were then resolved on the HPLC gradient of Stephens et al. [18]. Closed symbols indicate [^{3}H], and open symbols indicate [^{32}P]. The additional Gro*P*Ins5*P* peak observed in GFP-MTMR3-expressing cells is indicated by a white arrow.

We also consider an alternative model, albeit a speculative one, in which phosphatase substrate would act as an allosteric activator of MTMR3 function that leads to vacuole formation. Without phosphatase activity there would be no "off switch" for this activation, and thus the observed phenotype with MTMR3 (C413S) would result from constitutive activation with respect to vacuole formation. This scenario would propose MTMR3 to be an effector of PtdIns3*P* or PtdIns(3,5)P_2 and raises the possibility that other Myotubularin family members may operate in a similar fashion.

Materials and methods

Cell culture and transfection

HeLa cells were incubated with Dulbecco's Modified Eagle Medium supplemented with 10% fetal bovine serum, 1% nonessential amino acids, and 1% penicillin/streptomycin at 37°C, 5% CO_2. A standard calcium phosphate precipitation method was used for transfection, resulting in 20%–40% of the cells expressing the transfected protein after 24 hr.

SF9 cells were incubated at 27°C in IPL-41 insect medium (Sigma, United Kingdom) supplemented with 10% fetal bovine serum, 2% yeastolate, fungizone (2.5 μg/ml), and gentamycin (50 μg/ml). All cell culture reagents were from Life Technologies, United Kingdom, unless stated otherwise.

Plasmids and strains

The open reading frame (ORF) for human *MTMR3* was amplified by polymerase chain reaction (PCR) from pBluescipt-KIAA0371 (cDNA, a kind gift of T. Nagase, Japan), cloned into the pGEMT vector, and sequenced. GFP-MTMR3 and HA-MTMR3 were generated by further subcloning the *MTMR3* ORF into mammalian N-terminal-tagging expression vectors pEGFP-C2 (Clontech) and pcDNA3.1-HA (a pcDNA3.1 [Invitrogen]-derived vector that was obtained by the insertion of a Kozak-sequence and an HA tag between the KpnI and EcoRI sites of the multiple cloning site). The full-length protein and a C-terminal deletion mutant including the phosphatase domain (1–488) were subcloned into pAcG2T (Pharmingen) for the generation of recombinant baculoviruses MTMR3 and MTMR3 (1–488), respectively. A point mutant was generated by site-directed mutagenesis (Quickchange, Stratagene) at the active site of MTMR3 with the primers 5′-CCGGTGCTAGTACACTCCT CAGATGGCTGGGAC-3′ and 5′-GTCCCAGCCATCTGAGGAGTG TACTAGCACCGG-3′, and the resultant phosphatase dead construct (C413S) was subcloned into pAcG2T and into pcDNA3.1-HA. A point mutant (C1174S) in the FYVE domain of MTMR3 was generated by site-directed mutagenesis with the primers 5′-CGAGTATGCAAGTCTT CCTATAGCAGCCTAC-3′ and 5′-GTAGGCTGCTATAGGAAGACTT GCATACTCG-3′ and was subcloned into pcDNA3.1-HA.

For expression in *S. cerevisiae*, the ORFs of *MTMR3* and *MTMR3(C413S)*, respectively, were subcloned into the yeast expression vector pUG36 (gift from Professor Johannes Hegemann (Heinrich Heine University Dusseldorf); U. Guldener and J.H. Hegemann, personal communication). The resulting constructs pUG36-MTMR3 and pUG36-MTMR3(C413S) were used to transform the following yeast strains: BY4742 Mat−α his3Δ1 leu2Δ0 lys2Δ0; ura3Δ0 and BY4742 *fab1::kanMX4* (Euroscarf, Frankfurt, Germany).

Electron microscopy

Transfected HeLa cells were fixed for 2 hr in either 2% paraformaldehyde or 2% paraformaldehyde/0.125% glutaraldehyde in 0.2 M phosphate buffer (PB) (pH 7.4). Cells were processed for ultracryomicrotomy as previously described [15]. In brief, cells were scraped gently with a rubber policeman, and cell pellets were washed four times with PB containing 50 mM glycine. Cells were then embedded in 10% gelatin, and after solidification at 4°C, small blocs were prepared and infused for 2 hr in 2.3 M sucrose. The blocs were frozen in liquid nitrogen on the appropriate specimen holders, and ultrathin cryosections were prepared with an ultracryomicrotome (Leica, Ultracut UCT or FCS, Wien, Austria) and a diamond knife (Drukker, Cuijk, The Netherlands). Sections were retrieved from the knife with a mixture of 2% Methylcellulose/2.3 M sucrose (vol/vol) and put on formvar-carbon-coated grids. Ultrathin cryosections were immunogold labeled with anti-HA or anti-GFP antibodies as described. Protein A gold conjugates were purchased from Dr. J. W. Slot (Department of Cell Biology, Utrecht University, Medical School, Utrecht, The Netherlands).

Baculovirus production, transfection, and protein production

Baculovirus production and transfection were carried out with the BaculoGold system (Pharmingen) according to the manufacturer's instructions. SF9 cells were used for amplification of virus and protein production. Infected Sf9 cells (3 × 15 cm dishes) were harvested after three days, washed, and resuspended in 5 ml lysis buffer (10 mM Tris [pH 7.5], 100 mM NaCl, 1 μM $ZnCl_2$, 1 mM DTT, and protease inhibitor cocktail [Sigma]) before breakage by probe sonication. The supernatant from a spin at 21,000 g for 15 min was then incubated with glutathione-

Figure 6

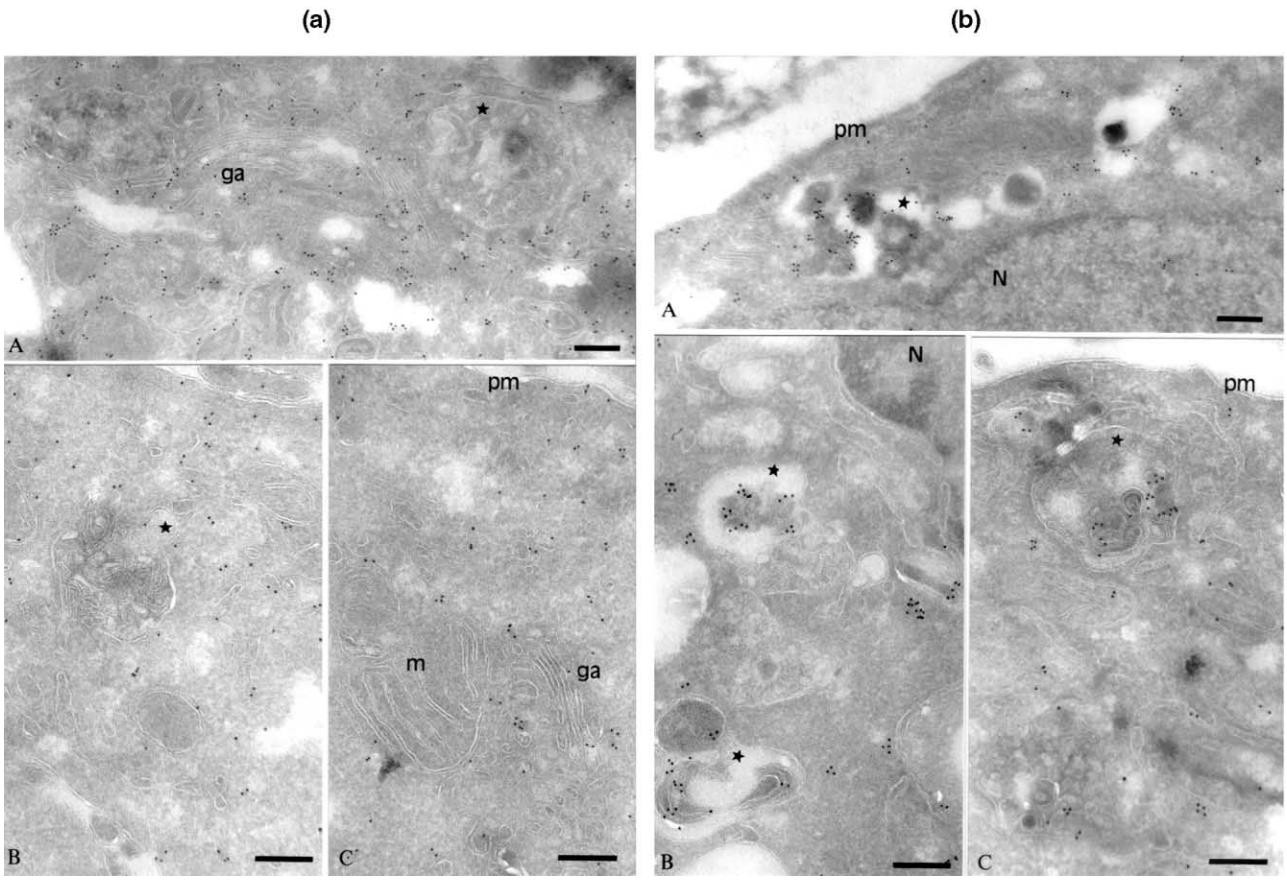

Electron-microscopic visualization of MTMR3 and MTMR3 (C413S) distribution. Ultrathin cryosections were labeled with the anti-HA antibody followed by protein A coupled to 10 nm gold particles (PAG 10). The scale bar represents 200 nm. **(a)** Immunogold localization of HA-tagged wild-type MTMR3 in HeLa cells. (a_A) Low-magnification picture showing the distribution of MTMR3 in a transfected cell. ($a_{B,C}$) Higher magnifications providing a more detailed view. The protein is enriched at the cytosolic face of membranes distributed throughout the cell; stars in (a_A) and (a_B) indicate multivesicular bodies. **(b)** Immunogold localization of HA-tagged MTMR3 (C413S) in HeLa cells. (b_A) Low magnification showing the localization of the mutant MTMR3 restricted to autophagic-like vacuoles. Note that the protein is poorly represented in the cytoplasm. ($b_{B,C}$) Higher magnifications showing examples of the autophagic-like organelles accumulating the mutant MTMR3. Stars indicate prominent examples of autophagic-like vacuoles.(Abbreviations are as follows: pm, plasma membrane; ga, Golgi apparatus; m, mitochondrion; N, nucleus.)

agarose (Amersham Pharmacia Biotech) before elution with 50 mM Tris-HCl (pH 8), 1 μM $ZnCl_2$, 10 mM reduced glutathione. The protein eluate was dialyzed overnight against 20 mM Hepes, 100 mM KCl, 1 μM $ZnCl_2$, and 0.2 mM DTT (pH 7.2).

Phosphatase assay

Phosphoinositide lipids (Cell Signals) were suspended in assay buffer (20 mM N-2-hydroxyethylpiperazine N′-2-ethanesulphonic acid [Hepes], 100 mM KCl, 1 μM $ZnCl_2$, and 2 mM DTT [pH 7.2]) at 2500 pmol per 50 μl per experimental point and shaken. The protein to be tested was added for the indicated time period, and the reaction was stopped by the addition of malachite green solution as previously described [3]. The reaction was measured by the change in absorption at 650 nm; appropriate controls were used.

Extraction and quantification of inositol lipids in yeast

Yeast strains were radiolabeled (10 μCi/ml [3H] *myo*-inositol) in 5 ml of inositol-free synthetic complete media lacking uracil and methionine (SC-Ura-Met) for 4–6 divisions (to a density of 2×10^6–4×10^6 cells/ml) at 30°C. Cells were either immediately killed by the addition of 2 volumes of ice-cold methanol:11.5 M HCl 100:1 (v/v) or treated with an equal volume of media plus 1.8 M NaCl for 10 min and then killed in the same manner. Dead cells were recovered from the methanol/media mixture by centrifugation, the supernatant was discarded, and the cells were broken by vortexing with glass beads (8×30 s vortexing with cells on ice for 30 s after every 30 s of vortexing) in 200 μl of methanol:11.5 M HCl 100:1 (v/v). Lipids were then extracted, deacylated, and resolved by anion exchange HPLC on a 25 cm Partisphere 5 μm SAX column, as described previously [9, 16–18] with the exception that 5 mM tetrabutylammonium hydrogen sulfate (Sigma) was included in the acid used to split the Folch mixture into two phases.

Synthesis of an authentic [^{32}P]GroPIns5P standard

[^{32}P]Gro*P*Ins(3,5)P_2 was isolated from [^{32}P]PO_4^{2-} radiolabeled yeast that had been stressed with 0.9 M NaCl for 10 min; total [^{32}P]radiolabeled lipids were extracted, deacylated, and resolved by HPLC, and the [^{32}P]Gro*P*Ins(3,5)P_2 peak was collected and desalted. [^{32}P]Gro*P*Ins(3,5)P_2 (500,000 dpm) was then treated with 0.7 ml of erythocyte ghost mem-

branes for 4 hr at 37°C in the presence of 5 mM EDTA and 1 mM EGTA (pH 7.5). The reaction was terminated by the addition of perchloric acid to a final concentration of 1 M, and then incubation of the acidified extract on ice for 15 min precipitated protein. The mixture was neutralized and desalted by the addition of 2 M KOH and 0.1 M Hepes, and incubation on ice for a further 30 min allowed salt precipitation. The precipitated protein and potassium perchlorate salt were then removed by centrifugation (15,000 × g for 15 min at 4°C). The supernatant was found to contain a 1:1:1 mixture of [^{32}P]Gro*P*Ins5*P*, [^{32}P]Gro*P*Ins(3,5)P_2, and [^{32}P]PO_4^{2-} as expected and was stored at −20°C until needed.

Imaging of yeast

Yeast strains were grown to a density of 1×10^6–2×10^6 cells/ml in SC-Ura-Met and concentrated 20-fold by centrifugation. Yeast were then viewed as unfixed, wet-mounted cells by the use of a Nikon E600 microscope with a Nikon 100×, DIC objective lens (1.4 numerical aperture). Images were then captured with an ORCA digital camera.

Supplementary material

Supplementary material including a discussion of immunofluorescence studies of MTMR3 localization, additional Materials and methods, and two supplementary figures is available at http://images.cellpress.com/supmat/supmatin.htm.

Acknowledgements

D.W. is the recipient of a Wellcome Trust prize studentship. S.U. is funded by the North West Cancer Research Fund. S.K.D. is a Royal Society Research Fellow. We thank T. Nagase for MTMR3 cDNA (KIAA0371). We also thank members of the Haematology Department, University of Liverpool for generous use of their confocal microscope.

References

1. Wishart MJ, Taylor GS, Slama JT, Dixon JE: **PTEN and Myotubularin phosphoinositide phosphatases: bringing bioinformatics to the lab bench.** *Curr Opin Cell Biol* 2001, **13:**172-181.
2. Hughes WE, Cooke FT, Parker PJ: **Sac phosphatase domain proteins.** *Biochem J* 2000, **350:**337-352.
3. Maehama T, Taylor GS, Slama JT, Dixon JE: **A sensitive assay for phosphoinositide phosphatases.** *Anal Biochem* 2000, **279:**175-176.
4. Zhao R, Qi Y, Zhao ZJ: **FYVE-DSP1, a dual-specificity protein phosphatase containing an FYVE domain.** *Biochem Biophys Res Commun* 2000, **270:**222-229.
5. Yamamoto A, DeWald DB, Boronenkov IV, Anderson RA, Emr SD, Koshland D: **Novel PI(4)P 5-kinase homologue, Fab1p, essential for normal vacuole function and morphology in yeast.** *Mol Biol Cell* 1995, **6:**525-539.
6. Rameh LE, Tolias KF, Duckworth BC, Cantley LC: **A new pathway for synthesis of phosphatidylinositol-4,5-bisphosphate.** *Nature* 1997, **390:**192-196.
7. Sbrissa D, Ikonomov OC, Shisheva A: **PIKfyve, a mammalain otholog of yeast Fab1p lipid kinase, synthesizes 5-phosphoinositides.** *J Biol Chem* 1999, **274:**21589-21597.
8. McEwen RK, Dove SK, Cooke FT, Painter GF, Holmes AB, Shisheva A, *et al.*: **Complementation analysis in PtdInsP kinase deficient yeast mutants demonstrates that Schizosaccharomyces pombe and murine Fab1p homologues are phosphatidylinositol 3-phosphate 5-kinases.** *J Biol Chem* 1999, **274:**33905-33912.
9. Dove SK, Cooke FT, Douglas MR, Sayers LG, Parker PJ, Michell RH: **Osmotic stress activates phosphatidylinositol-3,5-bisphosphate synthesis.** *Nature* 1997, **390:**187-192.
10. Cooke FT, Dove SK, McEwen RK, Painter G, Holmes AB, Hall MN, *et al.*: **The stress-activated phosphatidylinositol 3-phosphate 5-kinase Fab1p is essential for vacuole function in *S. cerevisiae*.** *Curr Biol* 1998, **8:**1219-1222.
11. Seglen PO, Bohley P: **Autophagy and other vacuolar protein degradation mechanisms.** *Experientia* 1992, **48:**158-172.
12. Kim J, Klionsky DJ: **Autophagy, cytoplasm-to-vacuole targeting pathway and pexophagy in yeast and mammalian cells.** *Annu Rev Biochem* 2000, **69:**303-342.
13. Petiot A, Ogier-Denis E, Blommaart EF, Meijer AJ, Codogno P: **Distinct classes of phosphatidylinositol 3-kinases are involved in signaling pathways that control macroautophagy in HT-29 cells.** *J Biol Chem* 2000, **275:**992-998.
14. Kihara A, Noda T, Ishihara N, Ohsumi Y: **Two distinct Vps34 phosphatidylinositol 3-kinase complexes function in autophagy and carboxypeptidase Y sorting in Saccharomyces cerevisiae.** *J Cell Biol* 2001, **152:**519-530.
15. Raposo G, Kleijmeer MJ, Posthuma G, Slot JW, Geuze HJ: **Immunogold labeling of ultrathin cryosections: application in immunology.** In *Handbook of Experimental Immunology*, vol. 4. Edited by Herzenberg LA, Weir D, Herzenberg LA, and Blackwell C. Cambridge, Massachusetts: Blackwell Science Inc.; 1997:1-11.
16. Dove SK, Michell RH: **Analysis of the phosphorylated inositol lipids of S. cerevisiae.** In *Signal Transduction: A Practical Approach*. Edited by Milligan G. Oxford, United Kingdom: Oxford University Press; 1999:255-281.
17. Hughes W, Woscholski R, Cooke F, Patrick RS, Dove SK, Macdonald NQ, *et al.*: **SAC1 encodes a regulated lipid phosphoinositide phosphatase, defects in which can be suppressed by homologous Inp52p and Inp53p phosphatases.** *J Biol Chem* 2000, **275:**801-808.
18. Stephens L, Hawkins PT, Downes CP: **Metabolic and structural evidence for the existence of a third species of polyphosphoinositide in cells: D-phosphatidyl-*myo*-inositol 3-phosphate.** *Biochem J* 1989, **259:**267-276.